

UNCLASSIFIED
AD 418210

DEFENSE DOCUMENTATION CENTER
FOR
SCIENTIFIC AND TECHNICAL INFORMATION
CAMERON STATION, ALEXANDRIA, VIRGINIA



UNCLASSIFIED

NOTICE: When government or other drawings, specifications or other data are used for any purpose other than in connection with a definitely related government procurement operation, the U. S. Government thereby incurs no responsibility, nor any obligation whatsoever; and the fact that the Government may have formulated, furnished, or in any way supplied the said drawings, specifications, or other data is not to be regarded by implication or otherwise as in any manner licensing the holder or any other person or corporation, or conveying any rights or permission to manufacture, use or sell any patented invention that may in any way be related thereto.

CATALOGED BY DDC

418210

AS AD No.

418210

FTD-TT
63-320

64-3

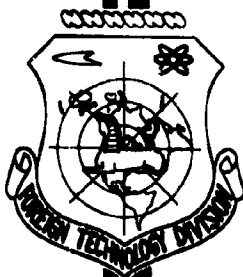
TRANSLATION

FREEZING OUT MOISTURE AND CARBON DIOXIDE
IN TUBULAR HEAT EXCHANGERS

By

G. V. Vasyunina and L. S. Aksel'rod

FOREIGN TECHNOLOGY DIVISION



AIR FORCE SYSTEMS COMMAND

WRIGHT-PATTERSON AIR FORCE BASE

OHIO

DDC
RECEIVED
OCT 1 1963
TISIA B

UNEDITED ROUGH DRAFT TRANSLATION

FREEZING OUT MOISTURE AND CARBON DIOXIDE IN
TUBULAR HEAT EXCHANGERS

BY: G. V. Vasyunina and L. S. Aksel'rod

English Pages: 36

SOURCE: Russian Book, Vsesoyuznogo Nauchno-Issledovatel'-
skogo Instituta Kislородnogo Mashinostroyeniya,
Apparaty i Mashiny Kislородnykh Ustanovok, Nr.
4, 1961, pp 184-207

S/800-61-0-4

THIS TRANSLATION IS A RENDITION OF THE ORIGINAL FOREIGN TEXT WITHOUT ANY ANALYTICAL OR EDITORIAL COMMENT. STATEMENTS OR THEORIES ADVOCATED OR IMPLIED ARE THOSE OF THE SOURCE AND DO NOT NECESSARILY REFLECT THE POSITION OR OPINION OF THE FOREIGN TECHNOLOGY DIVISION.

PREPARED BY:

TRANSLATION DIVISION
FOREIGN TECHNOLOGY DIVISION
WP-AFB, OHIO.

FREEZING OUT MOISTURE AND CARBON DIOXIDE IN
TUBULAR HEAT EXCHANGERS

G. V. Vasyunina and L. S. Aksel'rod

Symbols

α = heat-transfer coefficient;
 β = mass-transfer coefficient;
 γ = gas density;
 C_p = gas heat capacity;
 a = gas thermal diffusivity;
 D = vapor diffusion coefficient;
 dQ = amount of heat;
 dG = amount of substance;
 df = surface;
 p_2 = vapor pressure in the flow core;
 p_s = saturated vapor pressure;
 T_g = gas temperature;
 T_w = wall temperature;
 T_1 = gas temperature at the inlet;
 T_2 = gas temperature at the outlet;

c_g = concentration of vapor in the flow core;

c_w = concentration of vapor at the wall;

c_n = concentration of vapor during saturation;

$\epsilon = \frac{\alpha}{p\gamma_0 p}$ = Lewis coefficient;

S = degree of supersaturation of gas;

K_t = linear heat-transfer coefficient;

α_1 = coefficient of heat transfer from the wall to the cooling gas;

α_2 = coefficient of heat transfer from the cooled gas to the wall;

α_f = coefficient of heat transfer from the gas to the frost layer;

K_f = coefficient of heat transfer from the cooled gas to the wall;

λ_m = heat conduction of the tube;

λ_h = heat conduction of the frost;

λ = heat conduction of gas;

μ = viscosity coefficient;

d_1 = internal diameter of the tube;

d_2 = external diameter of the tube;

d_h = diameter of the frost layer;

t = step between the tubes;

H = distance between the baffles;

\underline{n} = number of tubes distributed with respect to the diameter;

g = unit load with respect to the frost;

g_s = standard unit load with respect to the frost;

τ = operating time of freezer until clogged;

τ_s = operating time of freezer until clogged when the unit is standard;

Re = Reynolds number;

Nu = Nusselt number;

Pr = Prandtl number;

G_w = gas weight flow;
 w = gas velocity;
 x_1 = initial moisture content of the air;
 x_2 = final moisture content of the air.

One of the methods of removing moisture and carbon dioxide from technological air flows is the freezing of these impurities in reversing heat exchanger-freezers serving simultaneously for cooling the air and heating the products of separation.

When designing freezers we should determine their thermal regime, design, and dimensions which guarantee the prescribed content of the frozen component at the outlet from the device for the prescribed duration of its operation up to clogging or switching.

Research [2, 4, 6, 9, 13, 14, 16, 17, 19] on freezing was conducted under various conditions which led, in most cases, to contradictory results and did not yield sufficient grounds for a true solution of the industrial problem.

This article reports the results of an experimental investigation of certain fundamental questions connected with the operation of moisture and carbon dioxide freezers in air separators.

Amount of Frozen Component at the Outlet From the Freezer

In order to determine the amount of impurities in the air beyond the freezers it is necessary to determine in what aggregate state they can be, depending on cooling conditions.

When the vapor-gas mixture moves over the cooling surface two processes take place simultaneously: heat transfer and mass transfer. Under appropriate conditions they can be accompanied by a change in the aggregate state of the vapor with its separation as a condensate

or in the form of crystals. In this work, in connection with freezers, we will examine the question of crystallization from the gaseous phase when the gas content in the vapor-gas mixture is small. When the wall is cooled to a temperature below the freezing point, equal or lower than the dew point in the cooled mixture, the vapor begins to change from the gaseous phase to the solid phase. We will call the crystals settling onto the cooling surface frost. As a result of cooling, the vapor content can correspond to undersaturation, saturation, or supersaturation at the mixture temperature. In the last case bulk crystallization is possible and the vapor-gas mixture will contain saturated vapor and aerosols, i.e., the crystals in the mixture under consideration, suspended in a volume, in the future will be designated snow.

For normal operation of the devices located behind the freezers the presence of both snow and supersaturated vapor in the flow is undesirable.

The magnitude of the supersaturation is characterized by the degree of supersaturation S which is the ratio of the vapor pressure in the vapor-gas mixture to the saturated vapor pressure when the temperature of the mixture over the flat surface of the equilibrium phase[1]:

$$S = \frac{P_g}{P_s} \quad (1)$$

Bulk crystallization occurs at supersaturation which is equal to or greater than some critical supersaturation. The magnitude of critical supersaturation depends on the properties of the vapor-gas mixture, the cooling conditions, and the existence of crystallization nuclei in the flow; gas ions and suspended particles serve as these

nuclei. Depending on the conditions of the formation of the flow of gas mixture the presence of its bulk crystallization nuclei can be characterized principally by the absence of suspended particles and gas ions, the presence of gas ions, or the presence of suspended particles. The magnitude of critical supersaturation will differ for these three cases.

Critical supersaturation has its highest value for a mixture in which suspended particles and gas ions are absent. According to the data of a number of authors [1], in this case the vapor pressure in the flow at which bulk condensation or crystallization begins due to fluctuation of the molecules can be more than 8 times greater than the saturated vapor pressure and in the presence of suspended particles bulk crystallization can occur at very low supersaturation.

Although the separators remove dust from the air, nevertheless we cannot assume that crystallization nuclei are completely absent in the flow. Under these conditions the third case can occur.

Experimental investigations [1, 2, 4, 6, 11, 13, and 17] disclose, under certain cooling conditions of vapor-gas mixtures, the formation of snow in the volume of gas. Tests were made with various mixtures and at significant differences of temperature between the gas and the cooling surface. The operating conditions, however, of the freezers of air-separators differ from the conditions under which these tests were carried out and, therefore, require special study.

The nature of the course of the process of freezing out depends on the relation of the rate of heat and mass transfer.

In order to analyze the freezing-out process, Hausen [8] like other investigators, used Lewis' coefficient [12] which characterizes the ratio of these rates:

$$\epsilon = \frac{\alpha}{\beta \gamma c_p} \quad (2)$$

He examined the process with two fundamental assumptions:

1) the temperature difference between the gas and the cold wall is so slight that the vapor pressure change in this interval can be expressed by a linear dependence;

2) the vapor above the frost surface is saturated.

From the general equations of heat and mass transfer

$$dQ = \alpha (T_g - T_w) df; \quad (3)$$

$$dG = \beta (c_g - c_w) df \quad (4)$$

we obtained

$$c_g - c_w = \epsilon (c_{gs} - c_w). \quad (5)$$

When $\epsilon > 1$ there is more vapor in the mixture than corresponds to saturation, since the rate of mass transfer is too small compared with the intensity of the heat transfer. The gas is cooled quicker than the substance can precipitate onto the wall, which creates conditions for supersaturation; when the crystallization nuclei are inside the flow, snow is formed.

When $\epsilon < 1$ the gas contains less vapor than corresponds to saturation, since $\beta \gamma c_p$ is greater than α . So much of the crystallizing substance is brought to the wall that the amount of it remaining is insufficient for saturation. The formation of supersaturated vapor and when crystallization nuclei are present, the formation of snow in the volume is possible when $\epsilon > 1$. When $\epsilon \leq 1$ crystals can be formed only on the wall of the tube.

On the basis of the similitude theory for a laminar flow

$$\epsilon = \frac{\alpha}{D} \quad (6)$$

From the boundary layer theory and momentum theory Hausen found that at the critical Reynolds number.

$$\varepsilon = \left(\frac{a}{D}\right)^{\frac{2}{3}} \quad (7)$$

for a turbulent flow

$$\varepsilon = 1 + 1,5 \text{Re}^{-\frac{1}{4}} \left(\frac{a}{D} - 1\right) \left(\frac{a}{D}\right)^{-\frac{1}{4}}. \quad (8)$$

When the Reynolds number is increased, ε approaches unity. Hence, snow should not form in a turbulent flow.

From the literature data [9, 11, 13, 14, and 17] we see that on cooling of a laminar flow of the mixture air-water vapor having $\frac{a}{D} = 0.937$, and when the temperature differences are small, snow does not form; under the same conditions in the flow for an air-benzene mixture in which $\frac{a}{D} = 2.475$ the presence of snow was observed. When the temperature differences between the wall and the gas were high we sometimes observed the formation of snow in the air-water vapor mixture as well. The literature sources do not give grounds for evaluating the region of temperature differences in which Hausen's theoretical premises are valid.

His assumption of the linear dependence of saturated vapor pressure on temperature for water and carbon dioxide even within limits of engineering accuracy is fulfilled only for a difference of 4-5°. In the existing heat exchangers of air separations the difference in temperature between the cooled air and the wall can reach 20-30°. Therefore, at first glance Hausen's calculations are inapplicable to the operating conditions of the industrial freezers of air separators. However, taking into account the effect of a forming frost layer on the course of the process, one cannot admit that such a conclusion is

indisputable.

Until now the question of the effect of a frost layer was examined in the literature in relation to an investigation, during freezing, of the magnitude of the heat-transfer coefficient from the wall the gas [3, 6, 7, 10, 16, 18, 19 and 20], which will be examined later in great detail. Here we consider it necessary to emphasize that the formation of a frost layer also essentially changes the conditions of the very course of the freezing process.

As has already been noted in the literature [13, 16, 17] the fact here is not only that the projecting crystals greatly agitate the flow, while when the gas permeates through the frost layer the snow which precipitated in the coldest layers of the flow can lag (adhere) on them. The fact is that the surface temperature of crystals with the greatest projection into the flow at a certain distance from the wall is higher than the wall temperature (similar to that which occurs for the ribs of heat exchangers). Therefore, the actual difference of temperatures between their surface and the gas will be noticeably less than between the gas and the wall.

This circumstance noticeably expands the region of temperature differences for which Hausen's theoretical assumptions remain valid.

In order to explain the effect of the temperature difference and initial concentration on the course of the process of freezing out we made tests on two laboratory models. A glass model was tested at atmospheric pressure, and a metal model was tested at a pressure up to 7 atm (abs.). Assuming that $\frac{R}{D} = 1.3$ for an air-carbon dioxide mixture, i.e., close to the value of this ratio for an air-water vapor mixture (the freezers operate with turbulent flow of the gas), the tests were made with water vapor.

The visual model (Fig. 1) is a copper tube with an outside diameter of 10 mm, with a wall 0.5 mm thick and 1300 mm long in a glass tube 25 mm in diameter with an evacuated glass housing. Dry cooling air is fed into the copper tube, and the moist air being investigated is passed around its outside. The water vapor is frozen out on the outer surface of the copper tube. The different moisture content in the working flow at the input to the model was attained by mixing the dry air with the air which passed through the humidifier. In order to obtain the required temperature, most of the cooling air was first passed through a coil immersed in liquid oxygen. The temperature of the cooling flow was regulated by changing the level of the liquid oxygen in the housing of the coil and by adding warm air to the flow.

The temperature of the flows was measured at the input and output from the model by copper-constantan thermocouples mounted on the sleeves of the model. Diaphragms measured the amount of gas. The moisture content of the air at the inlet and outlet from the model was measured by a hygrometer with respect to the dew point.

We fed warm air into the model in the beginning of the test, and in order to reach the prescribed thermal conditions the necessary moisture content at the inlet to the model was established.

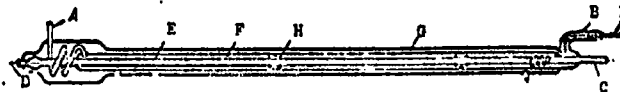


Fig. 1. Glass model of a freezer. A) inlet of cooled air; B) outlet of cooled air; C) inlet of cooling air; D) outlet of cooling air; E) copper tube; F) glass tube; G) evacuated glass housing; H) glass guides; I) thermocouple.

The air temperature at the inlet varied from +10 to +18°. The air was cooled to temperatures from +2 to -59°. The temperature difference of the air and the wall at the cold end varied from 15 to 140°. The moisture content of the air entering for cooling was calculated so that the dew point was different in the tests and varied from +3 to -18°. Table 1 shows the data of the tests.

TABLE 1

Data of the Tests Conducted on a Glass Model.

Test No.	Temperature of cooled air, °C		Velocity of air m/sec	Reynolds No. Re	Temperature differences between the gas and wall, °C		Dew point of cooled air, °C		Supersaturation
	at inlet	at outlet			warm end	cold end	at inlet	at outlet	
1	17,6	1,4	3,14	10750	18	13	-4,	-6,9	0,57
2	18,2	2,0	3,15	10700	18	18	-3,4	-6,2	0,5
3	15,0	-10,0	3,03	10700	28	27	-15	-20	0,4
4	15,0	-10,0	3,08	10700	28	27	+2,0	-10,0	1,0
5	17,2	-4,0	3,0	10200	29,6	26,4	-16,0	-30,4	0,08
6	16,2	-11,1	2,55	10000	40	39	-7,0	-16,0	0,63
7	17,0	-27,0	2,87	11500	49	56	-18,0	-31	0,47
8	10,3	-24,6	3,06	11210	59,3	67	-12,6	-28	0,71
9	18	-31	2,8	10700	62	58	+3	-18	5,1
10	14,5	-30,4	1,77	9450	63,5	64,3	-3	-15	4,7
11	18	-17	1,65	9430	70	81	+2,5	-11	1,47
12	18	-29	2,48	12820	73,5	92	-18,6	-28	1,1
13	15	-51,5	2,74	11300	118	111	-8,9	-17	4,7
14	12	-45	0,84	3620	135	115	-	-26	8,3
15	12	-42	2,83	12200	145	47	-12,8	-31	3,6

* Analyses were conducted immediately after feeding the moist air.

Three typical pictures of the course of the process of freezing out the moisture were observed visually, depending on the conditions of conducting the tests.

In the first case (tests No. 1-6), when the moist air was fed into the model the frost settled out only on the surface of the cold tube, while bulk crystallization was not observed. Analysis of the air for moisture content at the outlet from the model showed the absence of supersaturation.

In the second case (tests No. 7-12), at the moment the moist air was fed freezing out of the frost was observed on the cold tube as well as on the uncooled surface of the external glass tube; then the frost gradually disappeared from the glass wall and appeared no more. In this case we observed isolated snow crystals which precipitated on the conductors of the thermocouple, which were introduced into the working space of the model. Bulk crystallization was not detected with the naked eye, but analyses of a gas sample taken at the initial moment of feeding the moist air showed the presence of supersaturation.

In the third group (tests No. 13-15), when the moist air was fed into the model, snow formed in the flow; this snow was noticed along the entire length of the tube. At first the surface of the cold tube was covered with isolated crystals, and then frost began to gradually precipitate on it. As the amount of frost increased, the zone of snow formation shifted toward the cold end, and then the snow disappeared and the flow became transparent. It was visually observed that when the flow velocity significantly decreased and laminar regime was approached, the amount of snow in the flow increased.

The tests conducted on the model allow us to conclude that when freezing out moisture from air, and with a temperature difference between the gas and the glass tube of less than 30° we should not expect the formation of supersaturated vapor. In the case of a higher temperature difference when the moist air is fed during a certain period, the formation of supersaturated vapor and snow is possible. As a frost layer forms the zone of snow formation in these cases is curtailed, shifting toward the cold end of the apparatus, and after several minutes snow formation has already ended.

It should be noted that frost precipitates on all surfaces whose temperatures are below the dew point for the gas. For instance, in our first model, on the glass guides in the copper tube a great quantity of frost precipitated which most often caused clogging of the model. The temperature of the glass guides was obviously higher than that of the wall of the tube, but they appear to be stimuli to the agitation of the flow. During supersaturation, the snow also precipitates on the noncooled surfaces, e.g., on the thermocouple conductor.

The air velocity in the tests in which clear snow formation was not noted varied from 1.7 to 3.2 m/sec, and in this case separation of frost was not observed. When creating a pulsating flow the separation of frost from the walls was observed at the moment of a sharp increase of the velocity.

In all the tests the frost density along the length of the tube varied. According to visual observations at the warm end the frost was more dense, and toward the cold end of the tube its density decreased.

Tests with moist air at a pressure to 7 atm (abs.) were conducted on a metal model assembled according to the following diagram (Fig. 2). Dry clean air was fed into collector 1 from which it was removed both for feeding into the working tube 2 of model and for cooling. The part of the air fed into the working tube is first passed through humidifier 3 for saturation by water vapor, through moisture separator 4 for liberation from drops of water trapped by the flow, and is then mixed with the dry air entering from the collector. The amount of moist air and the total amount of air entering the tube was measured by precalibrated diaphragms. The temperature of the vapor-air mixture was first lowered somewhat in heat exchanger 5; then this mixture was

fed into the working tube of the model where it was finally cooled down to the prescribed temperature and released into the atmosphere through the regulating valve and the diaphragm. For cooling we used air fed from the collector, part of which went into coil 6 cooled by liquid oxygen. The temperature of the cooling flow at the inlet to the model was regulated by mixing the air cooled in the coil with the warm air (from the same collector). The diaphragm varied the amount of cooling air.

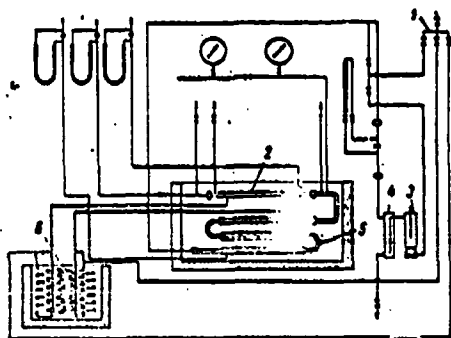


Fig. 2. Diagram of a metal model of a freezer. 1) air collector; 2) working tube; 3) humidifier; 4) moisture separator; 5) heat exchanger; 6) coil to cool the cooling air.

The freezer was made of copper tubing (Fig. 3) with an outside diameter of 18 mm, 3 mm thick, 1600 mm long, enclosed in a shell 20/25 mm in diameter. The vapor-air mixture was fed into the internal tube, and the cooling air into the external tube. The temperatures of the gas and wall were measured by the precalibrated copper-constantan thermocouples.

In order to measure the wall temperature, on the outer surface of the tube grooves were cut out into which the thermocouple junctions were put. The surface of the groove was first coated with glue to create an insulating layer. The thermocouple junction was fastened to the surface of the tube, and the leads were wound in several layers about the groove and covered by a thin protective film of electrical insulating material. The thermocouple junction and the leads were clamped to the wall by two brass half-rings on which we placed a

bushing, for strengthening, whose wall is 0.5 mm thick. There are grooves in the rings and bushing for passing the leads. The thermocouple leads were lead out of the model between the washers of the flanges. The gas temperature was measured by thermocouples mounted along the tube in those same cross sections where the wall temperature was measured (Fig. 4). We measured the emf by a PPTV-1 potentiometer.

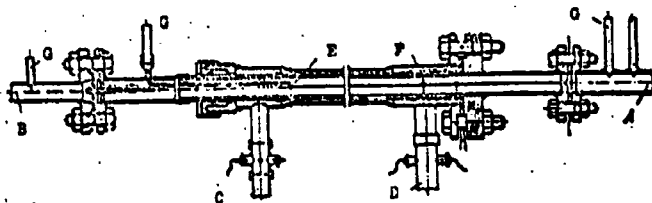


Fig. 3. Working tube of the metal model of the freezer. A and B) inlet and outlet of the cooled air; C and D) inlet and outlet of the cooling air; E and F) thermocouples for measuring the temperature of the gas and the wall; G) air specimen for analysis.

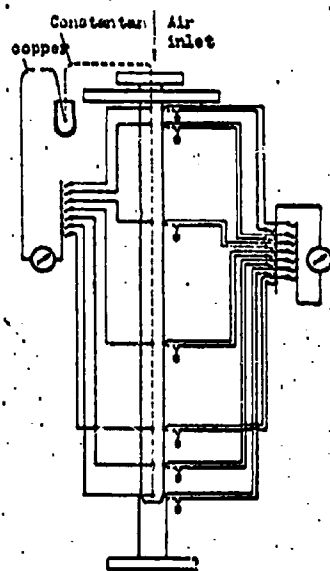


Fig. 4. Diagram of the position of the thermocouples in the working tube of the model.

The amount of water vapor in the air was determined by the dew point method using hygrometers. The air entering the model was analyzed at the input to the working tube. The cooled air was analyzed both at the outlet from the model and at a distance of 100 mm from the cold end. In order to prevent freezing, the analysis tube inside the model was provided with an electric heater.

At the beginning of the test the dry air was directed into the tube, and only after establishing the prescribed thermal regime was the moist air introduced.

The temperature of the air at the inlet in each test was held constant, and in different tests varied from +15 to -16°. The air was cooled to temperatures of -1 to -38°.

The difference in temperature between the gas and the wall of the tube in different cross sections did not exceed 30°. Table 2 shows the results of the analyses of the moisture content of the air at the outlet from the working tube of the model. In none of the tests did the analysis show the presence of supersaturated vapor. This same table also shows the values of the moisture content for each test, calculated by equations given in the literature.

TABLE 2

Test No.	Air pressure in the tube, mm Hg	Air temperature in the tube °C		Air velocity, m/sec	Reynolds number	Difference of temperature °C		Dew point °C			Super-saturation %	
		at inlet	at outlet			warm end	cold end	at inlet	at outlet	from calculation at the outlet	by analysis	by analysis
1	1.0	3.6	-20.2	4.13	3870	24.6	23.4	-28	-32.8	-31	0.61	0.5
2	1.0	5.0	-25	4.15	3870	23.8	21	-28	-32	-31	0.53	0.47
3	1.0	5.4	-25.2	4.15	3870	20.0	19	-13	-20	-20	1.7	0.92
4	1.4	4.8	-26	2.92	3800	23.8	20.2	-5.3	-20	-22	1.47	1.0
5	2.83	9.0	-25.2	3.25	8150	37.0	33.2	-32.0	-36	-35	0.34	0.32
6	2.83	7.4	-29.2	3.25	8150	32.4	28.8	-5.4	-29	-24.6	1.52	1.0
7	2.83	7.4	-28.2	4.43	11000	34.2	32.8	-16.7	-30.7	-29	0.91	0.77
8	3.83	8.7	-28.6	2.59	9140	33.7	35.6	-29	-36.7	-37	0.4	0.41
9	3.83	8.7	-24.8	2.59	9140	33.1	40.2	-20.9	-31.4	-28.6	0.68	0.51
10	3.98	10.3	-27.5	2.45	8550	35.7	35.3	-2.8	-28.4	-10.2	2.3	0.84
11	4.83	5.2	-25.6	2.68	11400	33.2	36.4	-26.7	-31.5	-33.2	0.46	0.54
12	4.83	7.1	-29.4	2.68	11400	32.1	32.6	-5.9	-29.2	-22.7	1.9	1.0
13	6.48	6.8	-22	2.02	11400	32	34.6	-4.6	-25.2	-18.7	1.4	0.71
14	6.48	6.6	-22.4	1.99	11500	31.8	35.6	-32.1	-34.2	-34.3	0.29	0.3

Amelin [1], in connection with the cooling of vapor-gas mixtures in coolers, derived, starting from the general equations of heat and mass transfer (3) and (4), an expression for determining the final vapor pressure when the temperature of the cooling surface is constant:

$$p_2 = \left(\frac{T_1 - T_w}{T_1 - T_w} \right)^{\frac{1}{2}} (p_1 - p_w) + p_w. \quad (9)$$

Linde [13] applied this same dependence to the case of freezing out vapor from the mixture.

With simultaneous solution of Eqs. (3) and (4) for the case when the temperature of the cooling wall is variable with respect to the length of the path of the gas, integration is possible only when the law of temperature change is known, and leads to cumbersome calculation operations. Therefore, when calculating we divided the surface, in accordance with the literature recommendations [1], one after another into a series of regions for each of which the temperature of the wall can, with sufficient accuracy, be considered fixed and equal to the average temperature in the region under consideration.

A comparison of the calculated data from Eq. (9) and the test data for regimes in which, according to the calculation, air nonsaturated or saturated by water vapor should be obtained at the outlet from the tube shows quite complete (within limits of the accuracy of the tests) coincidence of the values of the moisture content. In these same tests [3, 4, 6, 10, 12, and 13], in which by calculation supersaturated vapor or snow should have been obtained in the volume, analysis invariably showed a state of saturation at the outlet from the model. It should be pointed out that the air sample for determining the moisture content at the outlet from the model was chosen not at the first moment of feeding the moist air, but after a certain very short period of time.

The tests conducted with carbon-dioxide freezers, which we will discuss in detail below, showed that at the outlet from the apparatus

the CO₂ content, within limits of accuracy of the analysis, also corresponded to saturation.

Thus, the results of our tests show that the formation of a frost layer on the wall very rapidly changes the physical conditions of the process. As a result, the equations of type (9) proposed by Linde and other authors are proved inapplicable to calculating freezers as soon as the flow becomes saturated with vapor.

Under conditions of a thermal regime (and initial contents in the air of H₂O and CO₂ vapors the freezers of air separators in the case of the formation of a nonsaturated or saturated steam at the outlet we can make the calculations using Eq. (9). Here the surface of the heat exchanger is divided into a number of regions, in each of which we can assume the average temperature of the wall to be constant.

If calculation using Eq. (9) leads to supersaturation, then it is to be assumed, from Hausen's conclusions, that the amount of frozen-out component does not correspond to the final results of Eq. (9), but is equal to the equilibrium content with saturation.

Here the velocity of the gas should not exceed the rate at which separation of the frost from the wall is possible.

Heat Transfer Through the Surface Covered by Frost

With heat transfer through the clean wall of a tube, the linear thermal resistance is determined by the expression

$$\frac{1}{K_l} = \frac{1}{\alpha_1 d_1} + \frac{1}{\gamma \lambda_m} \ln \frac{d_2}{d_1} + \frac{1}{\alpha_2 d_2}. \quad (10)$$

If frost precipitates on the walls of the tubes (Fig. 5), the conditions of heat transfer vary owing to the appearance of an additional

thermal resistance and change of the magnitude and nature of the heat-transfer surface. Here, for instance, for a case of freezing on the external surface of the tube

$$\frac{1}{K_t} = \frac{1}{\alpha_1 d_1} + \frac{1}{2\lambda_m} \ln \frac{d_2}{d_1} + \frac{1}{2\lambda_f} \ln \frac{d_f}{d_1} + \frac{1}{\alpha_2 d_f} \quad (11)$$

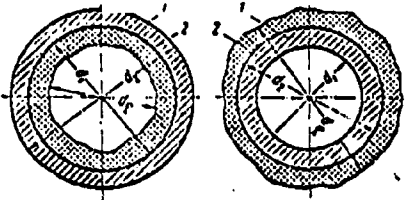


Fig. 5. Frost distribution in the tubes of the freezer: 1) wall of metal tube; 2) frost layer.

The coefficient of heat transfer from the wall to the coolant α_1 and the thermal resistance of the wall of the tube $\frac{1}{2\lambda_m} \ln \frac{d_2}{d_1}$ do not vary when frost appears and therefore can be disregarded for the present.

From previous works [6, 7, 16, 17, and 19] conducted by a number of authors it is known that the heat conduction of frost is a function of its density. The thickness of the frost layer $\frac{d_f - d_2}{2}$ depends both on the amount of precipitating substance and on its density.

As our experiments and literature data [4, 6, 8, 9, 13 and 17] indicate, the density of the frost layer depends on the nature of the process of its formation. When crystals are present in a volume of gas the frost layer consists not only of particles which formed on the wall but also those which precipitated from the gas flow on the frost crystals. In this case the frost layer will be less dense than when it precipitates only on the wall.

The hydrodynamic flow regime influences the structure of the frost precipitating on the walls. With laminar flow the frost is friable and porous. When the Reynolds number is increased the density of the layer increases, the roughness decreases, and the adhesive

force between the crystals and the wall increases. Inside the layer itself the density of the frost differs with thickness, and increases on approaching the wall. In the process of freezing, the average density of the frost increases with an increase in the amount of substance precipitating on the wall. When the vapor pressure is reduced, under conditions conducive to the growth of individual crystals, the density of the frost decreases.

When selecting the velocity of the vapor gas mixture in the freezer we should take into account the possibility of the crystals' breaking from the wall and being carried away with the flow.

In order to explain the effect of pressure on the magnitude of the flow velocity at which carry off begins, we conducted tests in a special model for the cooling of moist air at a pressure from 1.0 to 7 atm (abs.). The model (Fig. 6) is a tube with an outside diameter of 13 mm and 2.5 mm thick, in a housing 22/20 mm in diameter. We mounted a chamber at the cold end with two little windows to allow us to observe the flow. At the same place we extended the thermocouple leads for measuring the gas temperature. When the pressure is increased there is an increase in the velocity at which breakaway of the crystals begins which obviously, explains the greater density of the frost when the Reynolds number is increased. Thus, carrying away of the crystals was noticed at a pressure of 1 atm (abs.) for a velocity of 5.0 m/sec, while at a pressure of 7 atm (abs.) it was observed only for a velocity higher than 7.0 m/sec.

The abundance of factors influencing the frost structure also confirmed by our tests on the visual model, makes it difficult to explain the general dependences of frost density on the parameters of the process. Considering the variety of phenomena of the various

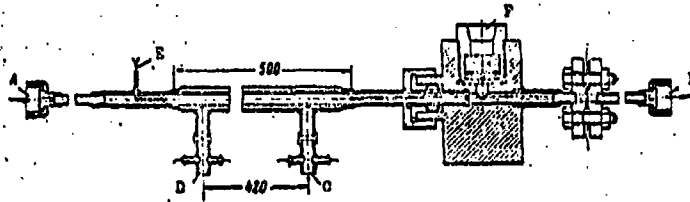


Fig. 6. Visual model for tests under pressure: A and B) inlet and outlet of the cooled air; C and D) inlet and outlet for the cooling air; E) thermocouples for measuring gas temperature; F) inspection window.

design factors in industrial freezers, there is hardly any sense in attempting a complete solution of this problem at present.

The specific density of the frost from water in the tests conducted for Reynolds numbers from 2300-14,000, according to the data of various authors [6, 7, 16, and 19], varied from 0.15 to 0.3 kg/dm^3 . The heat conduction of the frost from these same data is from 0.1 to 0.5 $\text{kcal}/\text{m}\cdot\text{hr}\cdot\text{deg}$.

When frost precipitates on the walls of the tubes the cross section for passage of air decreases, which leads to an increase of the velocity and, hence, to an increase of the coefficient of heat transfer from the air to the frost layer. If we do not take into consideration the permeation of the layer of crystals by the gas, then the heat transfer surface decreases when the frost precipitates inside the tube and increases when the frost precipitates on the outside of the tubes. The relations between the increase of the thermal resistance, the increase of the heat-transfer coefficient owing to the increase of the velocity, and the change in the magnitude of the heat-transfer surface depend on the design of the freezer and its hydrodynamic regime.

In order to estimate the change of the conditions of heat transfer due to the factors enumerated above, we can introduce the conditional total thermal resistance;

$$\frac{1}{K_f d_2} = \frac{1}{2\lambda_f} \ln \frac{d_f}{d_2} + \frac{1}{\alpha_f d_f} \quad (12)$$

For a clean wall $d_f = d_2$ and $\alpha_f = \alpha_2$.

The magnitude of the thermal resistance $\frac{1}{K_f d_2}$, depending on geometric factors, i.e., on the thickness of the precipitating layer, can be expressed as the function of the diameter of the layer surface d_f for constant thermal conductivity and constant gas parameters.

For instance, for freezing inside the tube we have the following dependence (Fig. 7):

$$\frac{1}{K_f d_1} = \frac{1}{\alpha_f d_f} + \frac{1}{2\lambda_f} \ln \frac{d_1}{d_f} \quad (13)$$

where

$$\alpha_f = \frac{Nu\lambda}{d_f}$$

For air we can assume [21]

$$Nu = 0.018 Re^{0.18};$$

$$Re = \frac{wd\gamma}{\mu g} = \frac{4G_v}{3600\pi\mu g} \cdot \frac{1}{d_f}$$

where G_v is the gas discharge in kg/hr.

Substituting the value of Re into Expression (13) we obtain

$$\frac{1}{K_f d_1} = \frac{d_f^{0.8}}{A} + \frac{1}{2\lambda_f} \ln \frac{d_1}{d_f}$$

where

$$A = 0,018 \left(\frac{4G_s}{3600\pi\mu g} \right)^{0,8} \lambda =$$

$$= 50,4 \cdot 10^{-7} \lambda \left(\frac{G_s}{\mu} \right)^{0,8}$$

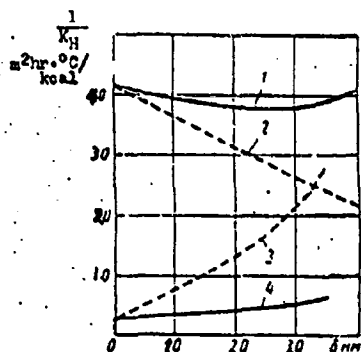


Fig. 7. The change in thermal resistance of heat transfer from the gas to the wall for precipitation of the frost

layer $\frac{1}{K_f} \cdot 10^2$: 1 and 2)

calculated data for the laboratory model of the freezer when $\lambda_f = 0.1$ kcal/m·hr·deg and $\lambda_f = 0.5$ kcal/m·hr·deg; 3 and 4) calculated data for the freezer under pressure when $\lambda = 0.1$ kcal/m·hr·deg and $\lambda = 0.5$ kcal/m·hr·deg.

compared to the original value α_2 for a clean wall. The graph in Fig. 7 gives the change $\frac{1}{K_f}$ as a function of the thickness of the frost layer of water δ for extreme values of λ_f

Curves 1 and 2 were calculated for a laboratory model of the freezer at a pressure of 1 atm (abs.); curve 3 and 4 were calculated for a freezer at a pressure of 150 atm (abs.).

For a cross flow in the intertubular space with a baffle when [22] $Nu = 0.25 Re^{0.6} Pr^{0.3}$ we obtain the function

$$\frac{1}{K_f d_2} = \frac{\left(\frac{t}{d} - 1 \right)^{0.6}}{A} + \frac{1}{2\lambda_f} \ln \frac{d_f}{d_2} \quad (15)$$

where

$$A = 0,25 Pr^{0,3} \lambda \left(\frac{G_s}{3600\pi\mu g} \right)^{0,8} = 43,3 \cdot 10^{-7} \lambda \left(\frac{G_s}{\mu} \right)^{0,8}$$

Analysis of Expressions

(13) and (14) as well as processing of test data using these expressions show that with the corresponding λ_f and α_f (the latter is not introduced in implicit form), both an increase and decrease of the value K_f can occur as

When freezing in a tube $d_1 = 10$ mm at 150 atm (abs.) of pressure, the initial heat-transfer coefficient α_f (until precipitation of the frost or for the flow of a clean gas) had a noticeably higher value than when testing at 1 atm (abs.) of pressure. Therefore, the appearance of additional thermal resistance has a more noticeable influence than a velocity increase. In tests at the same pressure of 1 atm (abs.) the effect of increasing the velocity prevails over the thermal resistance which causes an increase in K_f . For tests at a high pressure with significant magnitudes of the Reynolds number an increased value of the density should be expected, i.e., a higher value of λ_f . When freezing at 1 atm (abs.) of pressure the value λ_f will probably be closer to 0.1 than to 0.5; therefore, the curves for values of λ_f which are less probable, are plotted as dashed lines.

Magnitude K_f is also affected by the fact that when the frost freezes on the wall the heat-transfer surface becomes rougher than a surface of clean metal. As has been shown in papers on the study of heat transfer in tubes with different surface conditions [5, 15, and 16], when the roughness of the wall is increased the coefficient of heat transfer from gas to the surface can be increased up to three-fold as compared to its magnitude for a smooth wall. Thus, a certain increased value of α_f is possible depending on the surface condition of the frost. A combination of the effects examined above can (depending on the design and operating regime) lead to both an increase and a decrease of K_f as compared to a_2 .

According to experiments conducted previously [6, 7, 10, 16 and 17] K_f differs from a_2 in relatively restricted limits. According to certain test data K_f is somewhat higher than a_2 ; in most cases $K_f < a_2$, but not by more than two times.

It was noted that in most cases K_f at the beginning of the test decreases, and then its value remains constant.

When we conducted tests of models of the freezer and semi-industrialized test units the change of the magnitude of the heat-transfer coefficient K_f was miscalculated.

Processing of the test results showed that under operating conditions of the laboratory model there was no decrease in the magnitude of heat-transfer coefficient K_f compared with the initial value. In tests on the test unit of high pressure, about which more will be said below, it was noticed that when feeding the moist air the heat-transfer coefficient K_f decreased almost double, and then remained constant up to clogging the apparatus.

The thermal calculations of carbon-dioxide freezers did not show a noticeable change in K_f compared to α_2 . According to the calculations of the operating regimes of heat exchangers of the A-5400 nitrogen apparatus at the DATZ, the heat-transfer coefficient K_f during the operating period of the heat exchanger up to switching decreased by 25%.

Taking into account what was stated above and the difficulty of simulating the heat-transfer process during freezing, we can recommend, for air separators, that heat exchangers be calculated assuming the most severe conditions for heat transfer. With a certain margin we can recommend a value of K_f equal to one-half the initial magnitude of the calculated heat-transfer coefficient α_2 , i.e., $K_f = 0.5 \alpha_2$. Here, for low-pressure freezers a velocity of the cooled gas above 3.0 m/sec should not be used, in order to avoid separation of the frost from the walls.

The most important operating characteristic of the freezer is its continuous running time in a single operating cycle.

With freezing inside the tubes, an increase of the frost layer causes ever faster contraction of the channels for the flow of the vapor-gas mixture. Since the friction flow increases quadratically with an increase in the flow velocity, a relatively slow increase of the friction is observed for a certain time, and then it increases very rapidly to inadmissible values.

Figure 8 shows the calculated change of friction flow Δp when the channel diameter d is decreased by the frost deposit. Since the rate of diameter decrease increases with time, it is apparent that the clogging process will occur very rapidly.

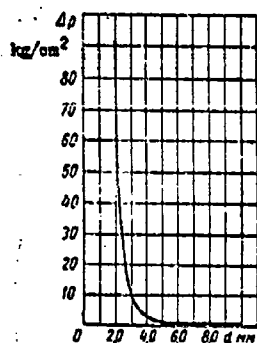


Fig. 8. Friction in the tube of the freezer.

During freezing in the tube space when frost precipitates during the initial period, the friction growth is also unnoticed, and then the friction smoothly increase to a limiting value.

The permissible continuous running time is limited by this increase of friction. The frost distribution along the operating channel can be irregular both with respect to the amount of the component being frozen out and

with respect to the density of the precipitate; therefore, clogging of the freezer can occur in separate most stressed regions. Calculation of the frost density, as has been pointed out above, is quite difficult. The quantitative distribution of the substance being frozen out along the heat-transfer surface can be determined in the first approximation by calculation on the basis of the conclusions of the

first section of this report. Therefore, in calculating the continuous running time of the freezers to clogging, we shall consider it advantageous to use the value of the unit load of the freezing surface with respect to frost g (the weight quantity of the component being frozen which is precipitating per unit of surface freezing of a clean tube).

The above data make it possible to consider that for two devices of identical (type) design with identical finite temperatures of the cooled flow, but differing with respect to output or operating length of the tubes, the running time to clogging is

$$\tau = \tau_e \frac{g_e}{g}, \quad (16)$$

where τ is the running time to clogging of the newly designed device;

g is the maximum unit load with respect to the frost in this device;

τ_e and g_e are the corresponding values for the test or the industrial device which we have at our disposal.

In order to verify these statements and to obtain initial data, during the calculations we experimented on testing units, on the freezing out of moisture from high-pressure air, on the freezing out of CO_2 from air at a pressure of 6 atm (abs.), and we investigated the operation of heat exchangers of the nitrogen device at the DATZ.

Tests on a High-Pressure Testing Unit

The testing unit is a system of spiral heat exchangers in which the premoistened air is cooled to the prescribed temperature (Fig. 9). Protection against cold losses and cooling of the counterflow was accomplished either by feeding liquid oxygen from the outside or by a high-pressure cooling cycle. The basic device of the testing unit,

the freezer was made from copper tube with an outside diameter of 15 mm, 2.5 mm thick, and 10 m long wound on a core. The tube was divided into 5-m sections connected in series. By means of a plug arrangement the second section can be cut out of operation. Two groups of tests were conducted; they differed in that at identical thermal loading, the heat-transfer surfaces were different.

We tested at an air pressure of 150 atm (tech.). Air in the amount of 43 kg/hr (in both tests it was saturated by water vapor) was cooled in the freezer from 4 to -30° .

In the tests with a tube 5 m long the temperature at the warm end was 37°C . The freezer clogged 23 hours after feeding of the moist air. In the tests with a tube 10 m long the temperature difference at the warm end was equal to 15° . The freezer was clogged after 70 hours. The resistance of the freezer did not increase gradually with time but increased very rapidly to ~ 50 atm (tech.). The moisture content of the air determined by a DDN-1 high-pressure hygrometer corresponded to saturation by water vapor for the temperature of a straight flow at the cold end, i.e., the dew point was equal to the gas temperature.

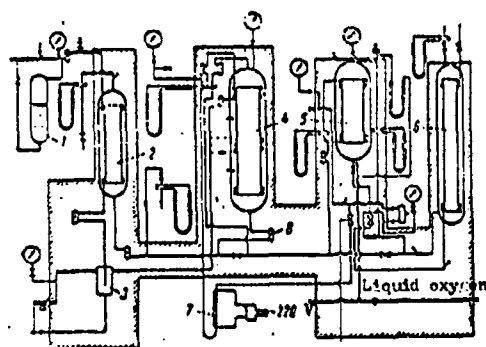


Fig. 9. Diagram of the testing unit freezing out of moisture under high pressure. 1) humidifier 2) liquifier; 3) moisture separator 4) freezer; 5) heat exchanger; 6) high-pressure heat exchanger; 7) heater 8) thermocouples for measuring the gas temperatures.

Assuming that in each cross section of the freezer the water vapor is in the saturated state, we constructed curves of the change in moisture content of the air along the tube (Fig. 10). The difference of the moisture contents at the inlet and outlet for each section of the tube characterizes the amount of water precipitating on the wall. For calculation we used sectors of a tube 0.5 m long, we determined the unit loads

$$g_{0.5} = G_v \frac{x_1 - x_2}{F_{0.5} \cdot 1000} \text{ kg/m}^2\text{hr},$$

and we constructed curves of their change along the device.

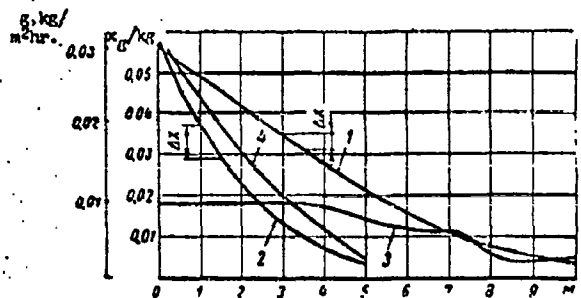


Fig. 10. The change in moisture content of air and the unit load along the freezer tube; 1 and 2) moisture content of air x in grams of water per Kilogram of air for tube lengths of 10 and 5 m; 3 and 4) unit load with respect to frost g in kilograms of water per m^2 of tube per hour for tube lengths of 10 and 5 m.

As is apparent from the calculation, for a 10-m tube the frost is distributed rather uniformly over the entire surface. At the warm end of the freezer, at a length of 4 m, the unit load is constant and is maximum: $g_{10} = 0.01 \text{ kg/m}^2\text{hr}$.

With a tube 5 m long a greater quantity of frost precipitates at the warm end than along the entire length of the device. The maximum unit load is equal to 0.03 kg/hr . The ratio of the maximum unit loads at the warm end of the freezer is

$$\frac{g_{5.0}}{g_{10}} = \frac{0.03}{0.01} = 3$$

Hence, with identical amounts of moisture entering the freezer, with a tube 10 m long the running time of the device until it clogs should be 3 times that of a tube 5 m long, which was confirmed by the test data.

Freezing Out of Carbon Dioxide and Low-Pressure Moisture

When testing the unit of the regenerators with an air sample from the middle we obtained data on the operation of tubular switching CO_2 freezers. In the freezers the compressed air with 0.03% CO_2 was cooled from -100° to -160° . The greatest temperature difference between the air and wall was 15° . Two freezers were mounted on the test unit (Fig. 11); they had tubes with outside diameters of 10mm, 1mm thick, and a pitch of 13 mm. The operating length of the tubes was 3222 mm. In one of the freezers the air was cooled in the intertube space (Fig. 12) equipped with baffles, and in the other it was cooled in the tubes.

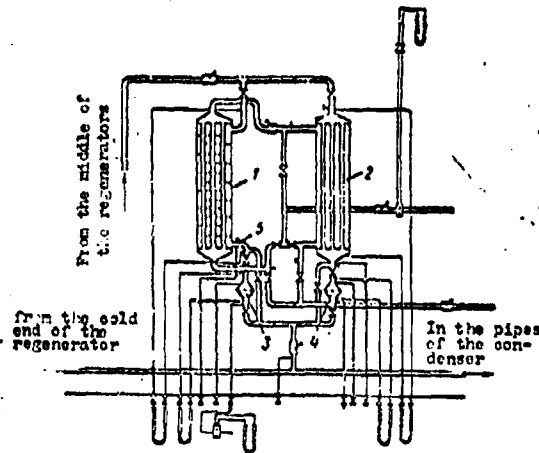


Fig. 11. Diagram of the operation of the freezer: 1 and 2) freezers with feeding of impure air into the intertube and tube space; 3 and 4) filters; 5) thermocouples for measuring the gas temperatures.

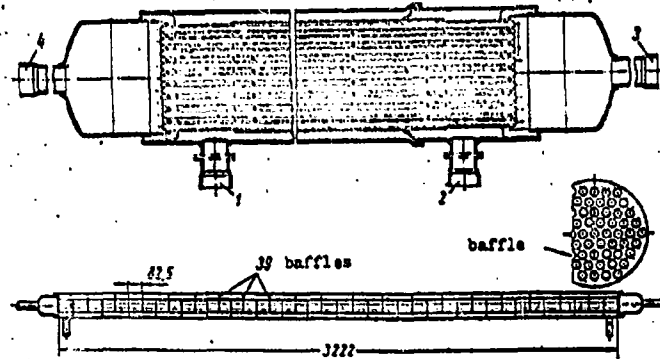


Fig. 12. Carbon dioxide freezer: 1 and 2) inlet and outlet of the cooled air; 3 and 4) inlet and outlet of the cooling air.

In the first freezer, analyses showed the CO_2 content to be close to saturation; in the second it was noticeably higher (Table 3). For the indicated temperature difference and with turbulent regime the formation of supersaturated vapor was not to be expected. The increased CO_2 content was apparently caused by the breakaway of the frost from the walls with a noticeable increase of the air flow velocity when the regenerators are switched in. This assumption was confirmed by the increased resistance of the filter placed in the air flow at the outlet from the freezer. With freezing in the intertube space, the falling frost is retarded by the baffles. The running time of the heat exchangers with freezing in the intertube space with an increase in resistance to 0.1 kg/cm^2 is 48 hours.

Table 4 shows the data from a calculation of the resistance of the freezers when cooling the air in the intertube space, under the assumption that the thickness of the frost layer is uniform along the surface of the freezer and the specific gravity of the CO_2 frost is

equal to 0.5 kg/liter.

The average unit load was equal to 0.01 kg/cm².

TABLE 3

Straight flow pressure atm(abs)	Amount of straight flow, kg/hr	Amount of counter-flow, kg/hr	temperature °C						velocity of straight flow kg/hr	Heat-transfer coefficient of a straight flow kcal/m ² hr °C	Heat transfer coefficient kcal/m ² hr °C	Heat-transfer coefficient kcal/m ² hr °C	CO ₂ content at the outlet, microportions	
			Straight flow			Reverse flow							at saturation	by analysis
			inlet	outlet	inlet	outlet	inlet	outlet						
Freezing in the tubes														
5.8	76.4	71.2	-80	-151	-105	-176	0.53	26.5	25.5	13	11.0	25.0		
5.8	90.6	71.8	-87	-152	-105	-175	0.68	38.4	31.0	16.0	9.0	27.0		
5.4	90.6	80.7	-95	-159	-116	-175	0.61	26.0	20.8	11.5	2.0	10.0		
5.2	91.5	87.5	-100	-158	-127	-175	0.67	29.3	29.0	14.6	2.7	7.0		
4.9	82.9	88.7	-102	-160	-132	-175	0.62	28.7	28.8	14.3	1.6	8.0		
4.5	57.5	46	-93	-153	-106	-176	0.5	19.1	10.9	7.0	9.0	25.0		
Freezing in the intertube space														
4.3	91.2	70.0	-102.5	-152.5	-105	-177	1.17	82.6	35.5	33.2	0.9	0-1.0		
4.5	61.6	53.2	-97	-161	-101	-172	0.83	62.9	41.1	24.8	0.8	2.0		
4.5	61.3	44.5	-97	-160	-99	-178	0.84	63.5	31.9	21.2	1.6	5.0		
5.5	62.6	65	-92.5	-159	-95.6	-172	0.65	65.2	42.0	27.7	2.0	5.0		

TABLE 4

outside diameter of the tube with frost, mm	air velocity m/sec	Resistance of one running kg/cm ²	Total resistance kg/cm ²	Calculated time from the beginning of switching, hrs.	Resistance of the freezer measured at this time, kg/cm ²
10.0	0.8	0.00018	0.0047	0	0
11.0	1.21	0.000235	0.0094	18	0.01 0.01 0.033
12.0	2.4	0.00075	0.03	36	0.03 0.12
12.5	5.2	0.00284	0.1135	48	0.10
12.9	24.3	0.0466	1.624	—	—

When designing, assembling, and operating the water freezers we should take into account the fact that introduction of water drops with the vapor decreases the running time of the device. Therefore, we should take measures to prevent the carrying away of drops from

the moisture separators and pipes. Switching shell-and-tube moisture freezers were investigated at the Dneprodzerzinsk nitrogen-fertilizer plant. The moist gas was fed into the intertube space of the heat exchanger where it was cooled from $22-30^{\circ}$ to -17 to -20° . Under operating conditions the resistance of the heat exchanger in the course of 3-5 hours reached 0.2 kg/cm^2 . In this case the average unit load with respect to the frost was $0.05 \text{ kg/m}^2\text{hr}$. During careful blow-out of the moisture separators and communication every 15 minutes the resistance of the heat exchanger increased to 0.2 kg/cm^2 only after 10 hours of switching (Fig. 13).

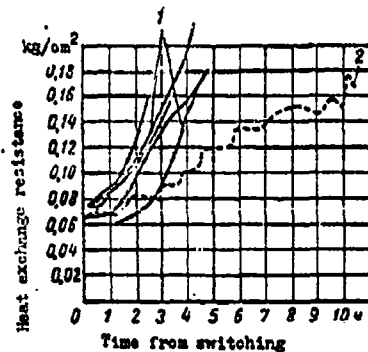


Fig. 13. Resistance change of A-5400 nitrogen heat exchanger: 1) heat exchanger resistance during normal operation; 2) heat exchanger resistance when blown out every 15 minutes.

Conclusions

1. During the process of freezing out moisture and carbon dioxide under the temperature conditions of the heat exchangers of air separators, the formation of bulk crystals is not to be expected.

At noticeable temperature differences (higher than 30°) crystal formation is possible at the initial moment of operation of the device, and then, during precipitation on the wall, fog formation gradually stops. Cooling the gas to the prescribed temperature with slight

temperature differences in a turbulent regime guarantees the presence of vapor in an amount not exceeding the equilibrium amount (corresponding to saturation) provided there is no breakaway of the frost from the walls.

To avoid breakaway of the frost the air velocity in the low-pressure freezers should not exceed 3.0 m/sec.

During freezing under conditions of a laminar regime with high temperature differences the formation of fog is possible for all mixtures. With small temperature differences and small initial concentrations of vapor the formation of fog depends on the physical properties of the mixture and is possible for mixtures in which $\frac{a}{D} > 1$.

2. The effect of the frost precipitating on the walls of the tubes on the intensity of heat transfer is a very complex function of the conditions of the process and the design characteristics of the device, and can lead to both a slight reduction and an insignificant increase in the intensity of heat transfer for freezing.

When designing new freezers it is advantageous that the heat-transfer coefficient for the flow of a vapor-gas mixture be twice as low as that calculated for a clean tube, and that the most unfavorable variant be taken into account and not lead to excessive reserves.

3. The running time of freezers of identical design depends on the magnitude of the maximum unit load with respect to the frost, i.e., the amount of frost precipitating on a 1 m² surface per unit time, corresponding to Eq. (16).

REFERENCES

1. A. G. Amelin. Teoreticheskiye osnovy obrazovaniya tumana v khimicheskikh proizvodstvakh, Goskhimizdat, 1951.
2. V. F. Gustov. Kristallizatsiya i vozgonka primesey v regeneratoryakh vozdukh-razdelitel'nykh ustanovok, Trudy VNIKIMASH, No. 1, 1956; No. 2, 1959.
3. K. Kan. Teplo- i massoobmen v vozdukhoolhaditele so spiral'nyimi rebrami, "Kholodil'naya tekhnika," No. 4, 1956.
4. K. A. Reznikovich. Issledovaniye protsessa kondensatsii vlagi v truboprovodakh i okhladitelyakh kompressornykh ustanovok. Dissertatsiya, Leningradskiy institut kholodil'noy i molochnoy promyshlennosti, 1951.
5. A. A. Seleznev. Vliyaniye sherokhovatosti na teplootdachu pri vynuzhdennoy dvizhenii zhidkosti. Dissertatsiya, Kazanskiy aviatsionnyy institut, 1954.
6. S. G. Chuklin. Teploperedacha i vlagoobmen v okhlazhdayushchikh sistemakh kholodil'nikov. Dissertatsiya, Moskovskiy khimiko-tekhnologicheskiy instityt im. D. I. Mendeleyeva, 1956.
7. K. O. Beatty, E. B. Finch and E. M. Shoenborn. Heat Transfer from Humid Air to Metal Under Frosting Conditions, Refrig. Eng., No. 59, No. 12, 1951.
8. H. Hausen. Einfluss des Lewisschen Koeffizienten auf das Ausfrieren von Dämpfen aus Gas-Dampf Gemischen, Angewandte Chemie (B.), Vol. 20, No. 7, 1948.
9. R. Hilz. Verschiedene Arten des Ausfrierens einer Komponente aus binären, strömenden Gasgemischen, Z. der Kälte-Ind., Bd. 47, No. 3, 5, 6, 1940.
10. E. Hofmann. Wärmeübergangsversuche an einem Plattenkühler unter besonderer Berücksichtigung der Reifschicht, Kalte No. 1, 1948.
11. A. P. Colburn, and A. G. Edisen. Prevention of Fog in Cooler Condenser, Ind. and Eng. Chemistry, Vol. 35, No. 4, 1941.
12. W. K. Lewis, The Evaporation of a Liquid into a Gas, Mech. Engr., Vol. 44, No. 27, 1922.
13. H. Lінде. Über das Ausfrieren von Dämpfen aus Gas-Dampf-Gemischen bei atmosphärischem Druck, Z. für Angewandte Physik, Bd. 2, Heft 2, 1950.
14. T. Mizushina. Mem. Fac. Eng. Kyoto Univ., Vol. 17, No. 2, 1955.

15. W. Nunner. Wärmeübergang und Druckabfall in luftdurchströmten rauhen Röhren, Chemie-Ing.-Technik No. 7, 1954.

16. L. Prins. Wärme- und Stoffübergang in einem querangeströmten bereifender Lüftkühler. Kältetechnik, Bd. 8, No. 6, 1956.

17. E. A. Rische. Ausfrieren von Dämpfen aus Gas-Dampf-Gemischen bei erzwungener Rohrströmung, Chemie-Ing. Technik, 29, No. 9, 1957.

18. E. Schmidt. Verdunstung und Wärmeübergang. Gesundheits Ingenieuren, Bd. 52, Heft 29, 1929.

19. K. Schropp. Untersuchung über Tau- und Reifbildung an Kühlrohren in ruhender Luft und ihr Einflue auf die Kälteübertragung, Z. der Kälte-Ind. Vol. 42. No. 5, 1935.

20. W. F. Stoecker. How Solid Deposit Affects Refrigeration Systems, Refrig. Engn. Vol. 65, No. 2, 1957.

21. M. A. Mikheyev. Osnovy teploperedachi, Gosenergoizdat, M. -L., 1956.

22. M. A. Kichigin, and G. N. Kostenko. Teploobmennyye apparaty i vyparnyye ustanovki, Gosenergoizdat, M. -L., 1955.

DISTRIBUTION LIST

DEPARTMENT OF DEFENSE	Nr. Copies	MAJOR AIR COMMANDS	Nr. Copies
		AFSC	
		SCFDD	1
		DDC	25
		TDBTL	1
HEADQUARTERS USAF		TDBDP	2
AFCIN-3D2	1	AEDC (AEY)	1
ARL (ARB)	1	BSD (BSF)	1
		AFPTC (FTY)	1
		ASD (ASYIM)	2
		SSD (SSF)	2
		ESD (ESY)	1
OTHER AGENCIES			
CIA	1		
NSA	6		
DIA	6		
AID	2		
OTS	2		
AEC	2		
PWS	1		
NASA	1		
ARMY (FSTC)	3		
NAVY	3		
NAFEC	1		
AFCRL (CRCLR)	1		
PGE	12		
RAND	1		